

10
11.12.40
94

Dr. 1974

MASTER

UCRL-52944

Energy deposition by high energy protons: comparison of theory and experiment

W. E. Loewe
C. W. Pollock

May 14, 1980

 Lawrence
Livermore
National
Laboratory

Energy deposition by high energy protons: comparison of theory and experiment

W. E. Loewe
C. W. Pollock

Manuscript date: May 14, 1980

DISCLAIMER

This code was developed in an account of work sponsored by an agency of the United States Government. Neither the United States Government nor any agency thereof, nor any of their employees, makes any warranty, express or implied, or assumes any legal liability or responsibility for the accuracy, completeness, or usefulness of any information, apparatus, product, or process disclosed, or represents that its use would not infringe privately owned rights. Reference herein to a commercial product, process, or service by trade name, trademark, manufacturer, or otherwise, does not necessarily constitute or imply its endorsement, recommendation, or favoring by the United States Government or any agency thereof. The views and opinions of authors expressed herein do not necessarily state or reflect those of the United States Government or any agency thereof.

LAWRENCE LIVERMORE LABORATORY
University of California • Livermore, California • 94550

Available from: National Technical Information Service • U.S. Department of Commerce
5285 Port Royal Road • Springfield, VA 22161 • 36.00 per copy • (Microfiche \$3.50)

CONTENTS

| | |
|--|----|
| Introduction | 1 |
| Description of the HETC Computer Code | 1 |
| Description of Experiments | 2 |
| Comparison of Calculated and Measured Data | 2 |
| Summary of Comparisons | 20 |
| Conclusions | 27 |
| Acknowledgments | 27 |
| References | 27 |

Energy deposition by high energy protons: comparison of theory and experiment

ABSTRACT

The ability of the HETC computer code to calculate energy deposited by proton beams of 0.8 to 28.5 GeV in composite targets was evaluated by comparing calculated results with experimental data. The experimental assembly consisted of ^{238}U shower plates separated by an air gap from a $\text{CH}_2/^{238}\text{U}$ detector plate. For protons in the range 0.8 to 5 GeV, HETC data on energy deposited can be considered accurate to a few tens of percent or better for the shower-plate part of the assembly and to better than fifty percent for the moderator/detector plate. The calculated fission density data may be assumed to be of similar quality. At higher energies, HETC data must be used with caution, but not suspicion. Because these assemblies provide a severe test of the calculational model, and in view of the overall quality of the comparisons, the agreement between measured and calculated values may be judged excellent, and serves as an absolute validation of the values quoted here for energy deposited in such physical configurations.

INTRODUCTION

The purpose of the work reported here was to evaluate the ability of the HETC computer code¹ to calculate energy deposited by GeV proton beams in composite targets.

HETC is a Monte Carlo high-energy nucleon transport code developed by Oak Ridge National Laboratory (ORNL). We obtained it from the ORNL Radiation Shielding Information Center (RSIC) and adapted it to the LTSS* computer system, which is used on Livermore's CDC 7600 computers. A special version of the HETC post-

processor was supplied by T. A. Gabriel of ORNL.

Calculations were performed for an experimental configuration for which LLNL experimenters had previously measured energy deposition and fission densities during exposures to proton beams of 0.8, 2.1, 4.88, and 28.5 GeV.² This configuration, which was designed to emphasize effects dependent on the angular distributions of cascade particles, was composed of ^{238}U shower plates separated from a $\text{CH}_2/^{238}\text{U}$ detector plate.

DESCRIPTION OF THE HETC COMPUTER CODE

HETC models detailed interactions in three-dimensional space. Input modules are available for problems with cylindrical symmetry, as well as for fully three-dimensional problems. The desired information, such as energy deposited, is extracted from a history record written by HETC. HETC uses analog Monte Carlo tracking procedures, based on straight-line travel between collisions with nuclei, to

describe the motion of primary and secondary protons and of secondary neutrons, pions, and muons. Then it corrects the position and direction of the primary proton at the event sites with a conventional Gaussian representation of the cumulative effects of multiple small-angle scattering caused by electromagnetic interactions with atoms. HETC uses a stopping-power formula based on the continuous slowing-down approximation to determine energy loss along these straight-line segments.

*Livermore Time Sharing System.

Collisions with nuclei are calculated by Monte Carlo tracking within a graded-density nucleus composed of individual noninteracting nucleons. Particle-nucleon interaction probabilities are based on experimental data for free particle-particle cross sections, and secondary particles are tracked in turn. After the intranuclear cascade has finished, the residual nucleus is permitted to evaporate neutrons, protons, deuterons, tritons, alphas, and helium-3 nuclei. The emitted neutrons and protons are then tracked.

When a particle's energy exceeds 3 GeV, HETC obtains the energy, angle, and multiplicity of

secondary particles from a collision by extrapolating 3-GeV intranuclear-cascade data according to specified scaling relations. When a particle's energy is less than HETC's cutoff energy (20 MeV for protons, 18 MeV for neutrons, 2.9 MeV for charged pions, and 2.3 MeV for muons), HETC stops tracking that particle. Neutrons below 18 MeV are then tracked by linking to the conventional Monte Carlo code MORSE-L,³ which uses ordinary multigroup interaction cross sections. The remaining energy of any other particle is deposited at the point where it reached the cutoff energy. HETC always treats hydrogen as a special case.

DESCRIPTION OF EXPERIMENTS

Figure 1 shows the assembly used in the experiments selected for calculation. Proton beams a few centimeters wide impinged first on a 7-inch-square flat shower plate of ²³⁸U that was 4 inches thick. Fifteen inches beyond this shower plate was a 7-inch-square composite detector plate consisting of a 2-inch-thick polyethylene moderator followed by a 1/8-inch-thick ²³⁸U plate. Deposited energy was measured using small thermoluminescence dosimeters (TLD's) mounted in radial arrays on special plates located at various depths in the assembly. TLD plates were located on the front, in the middle, and on the rear of the uranium shower plate, on the front of the polyethylene moderator plate, and behind the uranium detector plate. In addition, induced fissions were measured as fission-fragment track densities in Lexan foils placed against every available uranium face. Finally, a ²³⁵U foil, covered with Lexan film and contained in ¹⁰B, was embedded in the back face of the uranium detector plate.

Beam energies of 0.8, 2.1, 4.88, and 28.5 GeV

were used. Beam intensities were measured using the ¹²C (p, pn) ¹¹C reaction in a thin polystyrene sheet placed in the beam. Radial profiles were characterized by the experimenters as Gaussian distributions fit to the area at half-maximum observed on the first TLD plate. Beam asymmetry may also be obtained from the first TLD plate, directly from the two-dimensional TLD array.

In the comparisons described in this report, beam asymmetry is evidenced on the TLD radial profiles that have been keyed according to angles from reference of 0°, 45°, 90°, and 135°. The data for these keyed displays were provided in especially convenient computerized form by W. E. Farley, a member of the experimental team. We have added color coding for emphasis to the displays of the 800-MeV data, which had the greatest beam asymmetry.

The experimenters assign an uncertainty of $\pm 15\%$ to the TLD measurements, and indicate factor-of-two uncertainties in the fission measurements.

COMPARISON OF CALCULATED AND MEASURED DATA

Because of the much smaller quoted uncertainties in the TLD measurements, this report compares deposited energy for all radial and axial locations, but includes only exemplary or summary comparisons of fission data.

No adjustments were made in the rad values that were read instrumentally, and no normalizations or parameter adjustments were made in

calculating the energy deposited (in rads*) by the measured number of incident protons at the specified beam energy. Although the beam asymmetry could have been modeled explicitly in the calculations, it was not.

*One rad equals 100 ergs per gram (0.01 joule per kilogram).

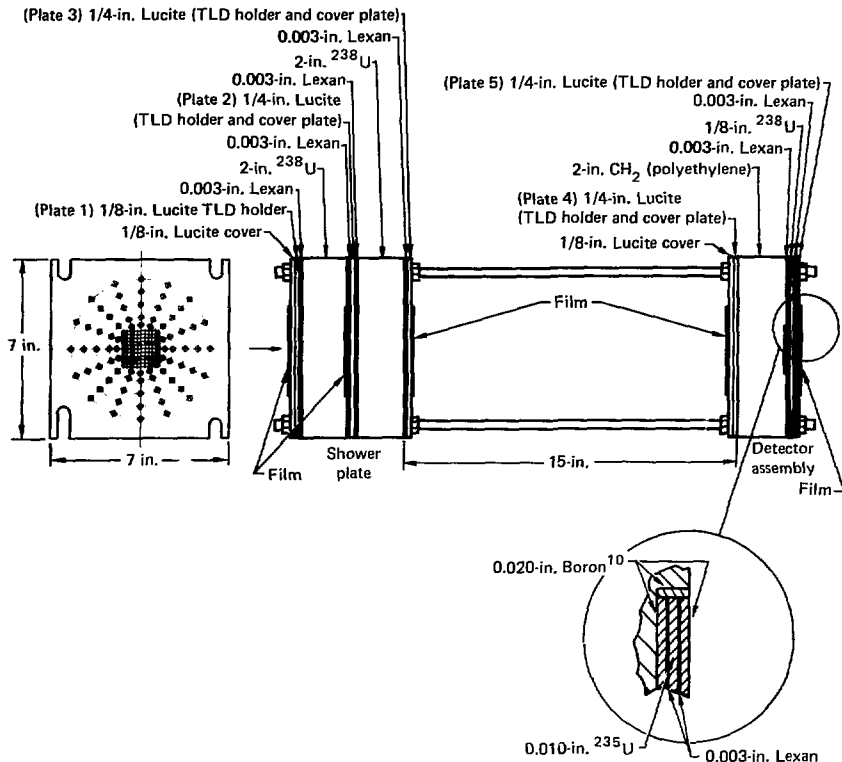


FIG. 1. Standard shower plate and detector assembly.

On-axis values of these calculated data cannot be given the emphasis ordinarily accorded maximum values, because they are a result of a compromise in radial zoning used to accumulate computational statistics. Thus, the innermost radial zone is too large for adequate definition, and underestimates the true axis value. (A better estimate of the calculated axis value could be obtained by extrapolating into zero radius a line connecting the midpoints of each step in the histogram.) At the same time, the innermost radial zone is too small to permit gathering adequate statistics at deep axial locations in a reasonable computer running time. Therefore, as the statistical quality worsens with

depth (due to losses of Monte Carlo particles out the sides as well as to interactions in the intervening material), the calculated on-axis values become somewhat unreliable. (This will be amplified later in the discussion of Table 2.)

800 MeV BEAM

The deposited-energy comparisons for the 800-MeV beam are shown in Figs. 2-6. The dose in rads, as indicated by TLD's and as calculated from the energy deposited by protons of the measured incident intensity, is plotted against the distance in centimeters from the maximum value at each TLD

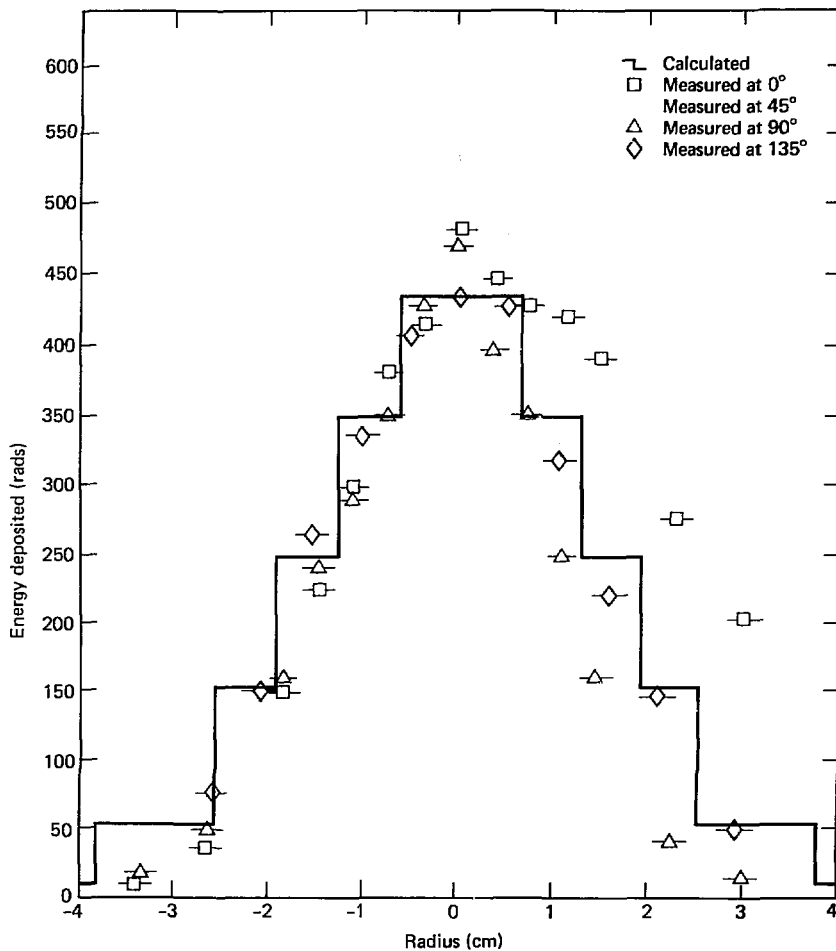


FIG. 2. Energy deposited by an 800-MeV proton beam on the front of the uranium shower plate assembly (TLD Plate 1).

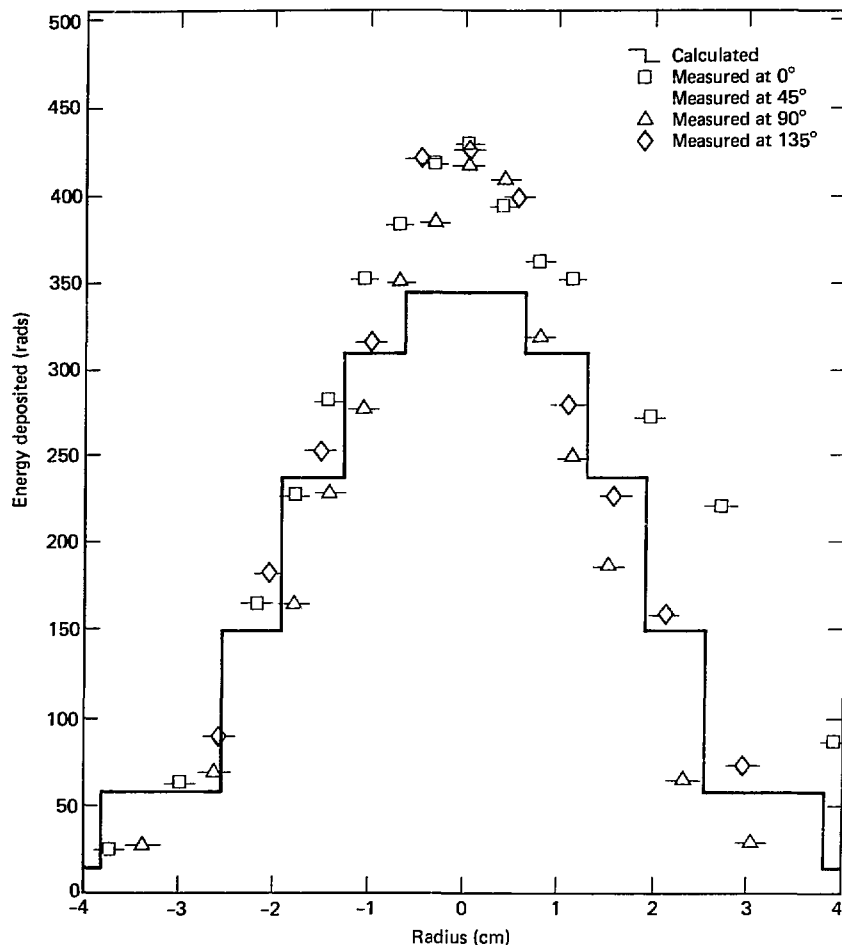


FIG. 3. Energy deposited by an 800-MeV proton beam in the middle of the uranium shower plate assembly (TLD Plate 2).

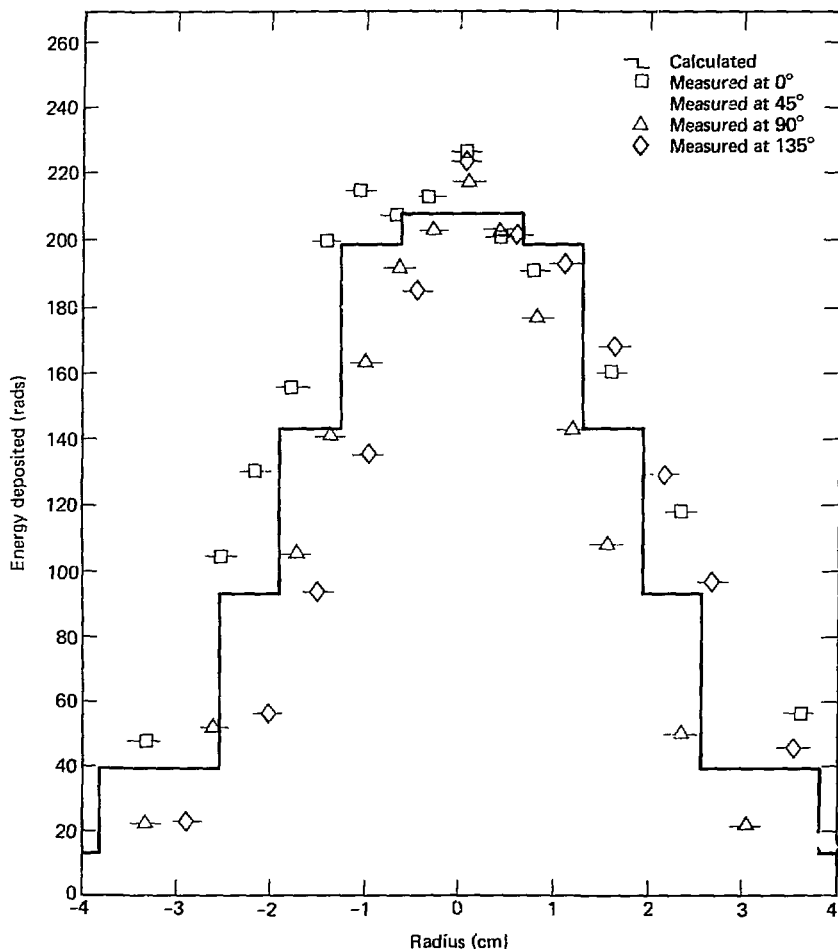


FIG. 4. Energy deposited by an 800-MeV proton beam at the rear of the uranium shower plate assembly (TLD Plate 3).

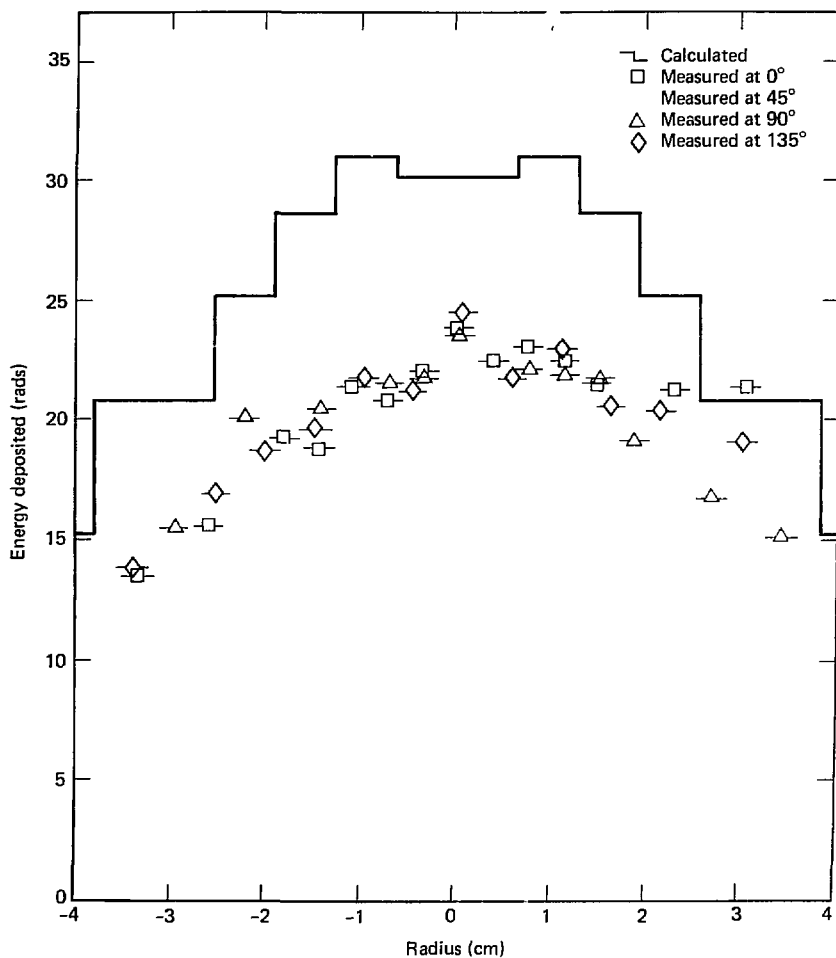


FIG. 5. Energy deposited by an 800-MeV proton beam on the front of the polyethylene moderator, behind the air gap (TLD Plate 4).

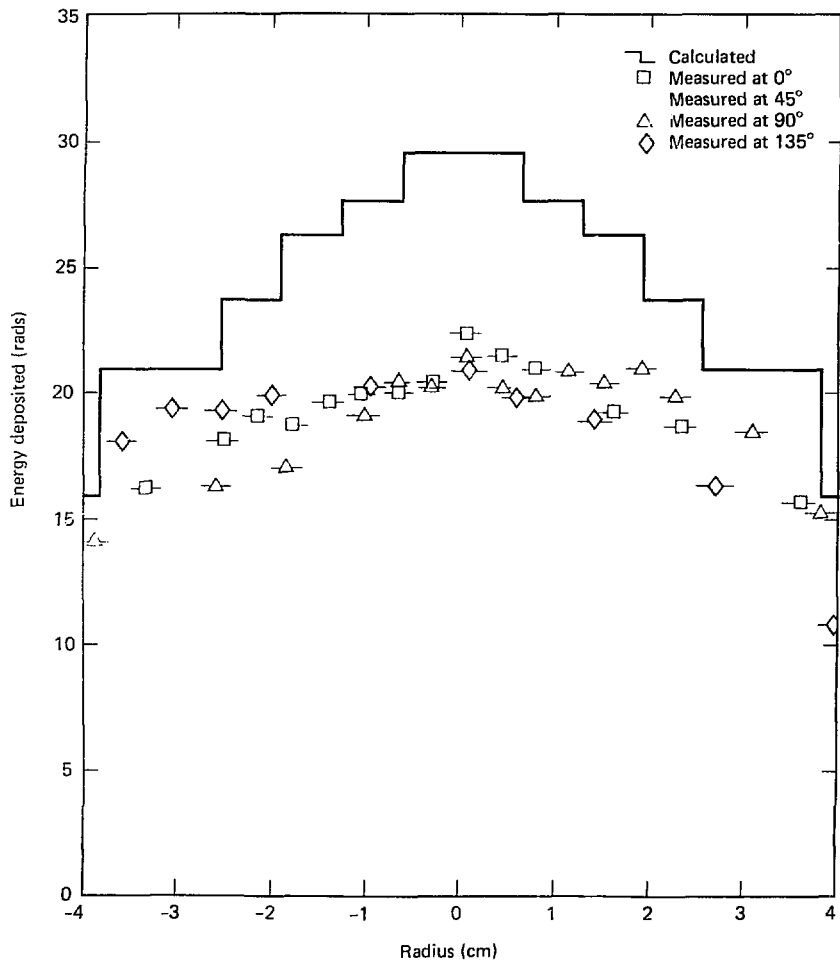


FIG. 6. Energy deposited by an 800-MeV proton beam behind the uranium detector plate (TLD Plate 5).

plate location. The TLD plates are numbered 1 through 5, beginning with Plate 1 on the front of the assembly.

The overall agreement in Fig. 2 establishes the accuracy of the beam calibration, since effectively no changes in the beam have taken place, and the energy deposition is the result of well-known stopping power mechanisms that have been incorporated into HETC exactly. Although we do not use one-sigma error bars, the statistical quality of the calculations can be inferred from the smoothness in the radial distribution.

The major features of Figs. 2-6 are: (a) very good radial profile agreement everywhere and very good amplitude agreement in front of the air gap, and (b) an amplitude discrepancy of roughly 40 to 50% immediately behind the air gap (shown in Fig. 5). This amplitude discrepancy, which is the subject of another report,⁴ strongly suggests some sort of modeling deficiency in HETC, such that the angular distribution of particles leaving the rear of the shower plate is slightly in error. Although we studied the multiple small-angle scattering model in HETC with considerable care, we did not find the approximations used to be sufficiently poor to explain this amplitude discrepancy. The cause of the discrepancy is therefore unknown.

Table 1 compares calculated and measured fission densities in (cal/g)/(kJ/m²), the units for specific density favored by the experimenters, for the 800-MeV beam. The agreement between calculated and measured values is surprisingly good, considering the quoted experimental uncertainties.

The fission-density calculations were made possible by changes to HETC, suggested by T. A. Gabriel of ORNL, that provide estimates of the number of fissions caused by nucleons with energies above the HETC cutoff (i.e., those fissions not a result of neutrons transported in the MORSE-L code). These estimates are based on the occurrence of nonelastic collisions as determined by HETC during particle tracking.

2.1-GeV BEAM

The deposited-energy comparisons for the 2.1-GeV beam are shown in Figs. 7-11. The discussion of the 800-MeV data is also appropriate here, with two exceptions. First, the beam asymmetry was much less for the 2.1-GeV beam than it was for the 800-MeV beam. Second, the statistical quality of the calculated 2.1-GeV data is somewhat poorer (fewer Monte Carlo particles were run). However, the same characterization of the comparison is valid. The loss of definition caused by the wide on-axis radial bin is more pronounced for the narrower 2.1-GeV beam.

4.88-GeV BEAM

The deposited-energy comparisons for the 4.88-GeV beam are shown in Figs. 12-16. The discussion of the two previous beam energies is also appropriate here, with the exception that the discrepancy between measured and calculated values at Plate 4 is only perhaps 30 to 40% instead of 40 to 50%. Furthermore, the discrepancy has been

TABLE 1. Fission energy, in (cal/g)/(kJ/m²), deposited on axis by a 0.8-GeV proton beam.

| Location | Calculated energy (C) | | | Measured energy (M) | Ratio, C _{total} /M |
|--------------------|--------------------------------|----------------------------------|----------------------|---------------------|------------------------------|
| | Induced by low-energy neutrons | Induced by high-energy processes | Total fission energy | | |
| A ^a | 0.094 | 0.159 | 0.25 | 0.20 | 1.3 |
| B ^a | 0.125 | 0.152 | 0.28 | 0.30 | 0.93 |
| C ^a | 0.116 | 0.121 | 0.24 | 0.22 | 1.1 |
| D ^a | 0.052 | 0.096 | 0.15 | — ^b | — ^b |
| E + F ^c | 0.0014 | 0.0079 | 0.009 | 0.01 | 0.90 |
| 235U foil | 0.0012 | (0.005) ^d | (0.006) ^d | 0.04 | — ^d |

^aLocations A, B, C, and D are on or in the uranium shower plate: A is at the front face, B and C are in the center, and D is at the rear face.

^bDatum not available.

^cLocation E + F is at the rear face of the detector plate.

^dInadequate statistical quality.

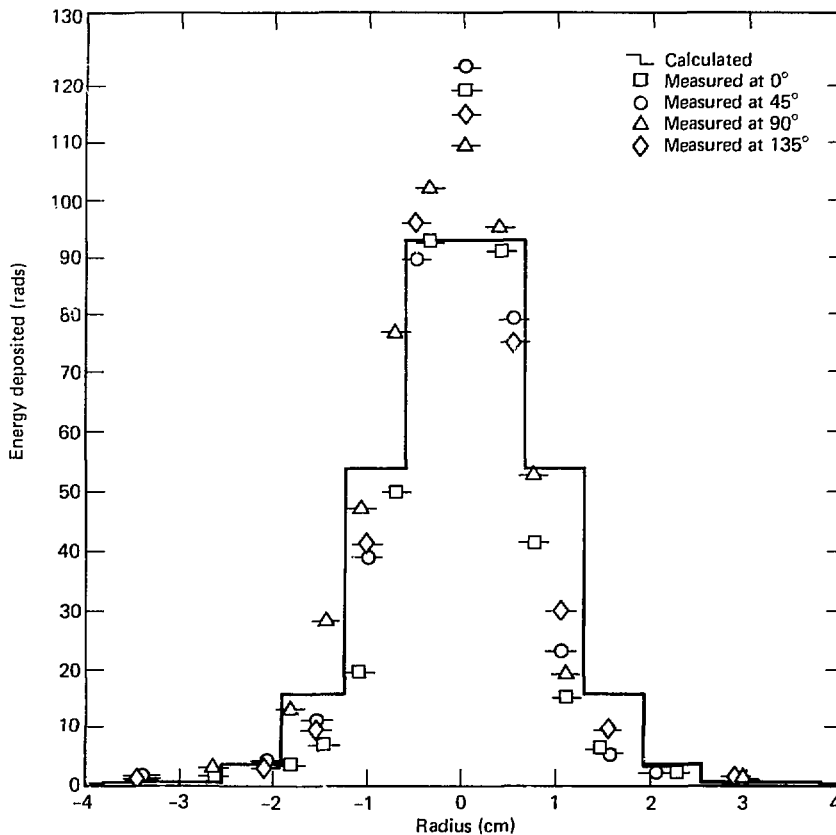


FIG. 7. Energy deposited by a 2.1-GeV proton beam on the front of the uranium shower plate assembly (TLD Plate 1).

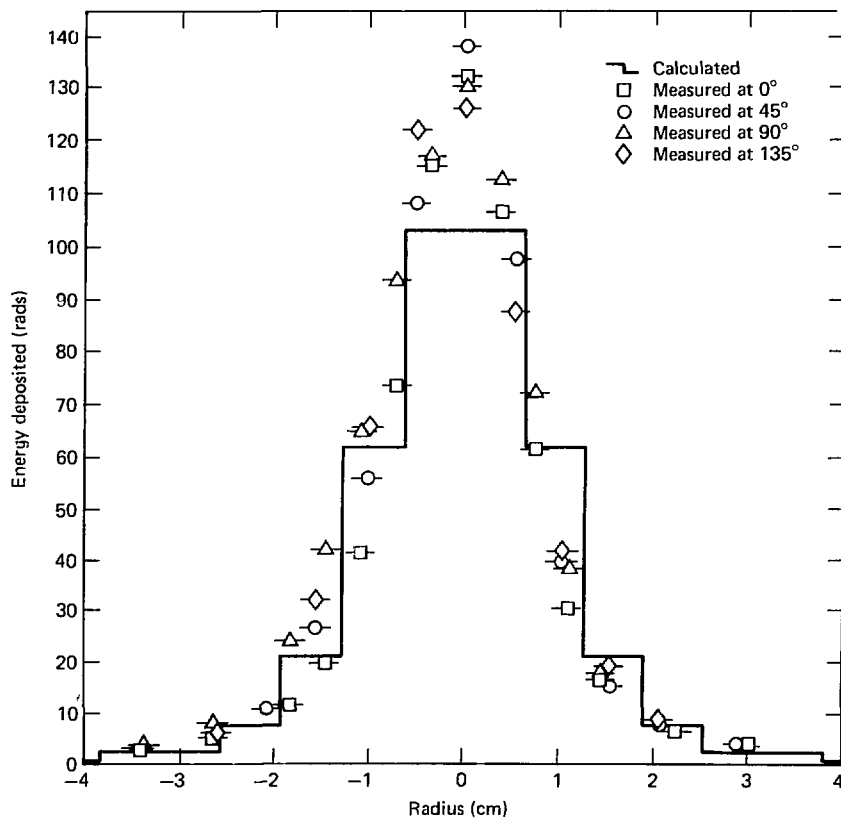


FIG. 8. Energy deposited by a 2.1-GeV proton beam in the middle of the uranium shower plate assembly (TLD Plate 2).

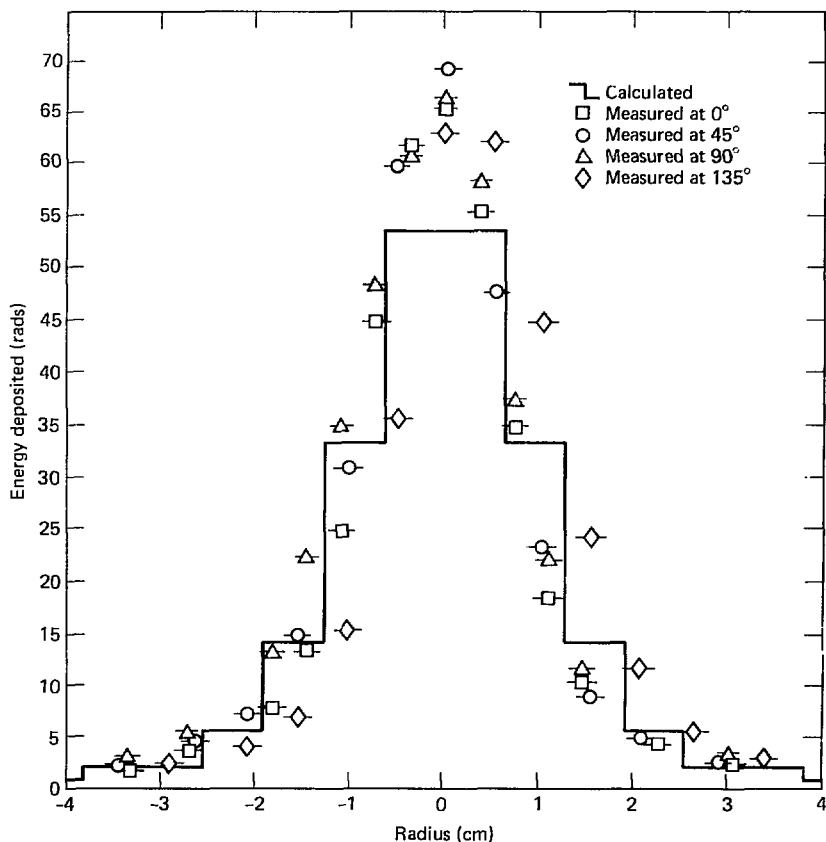


FIG. 9. Energy deposited by a 2.1-GeV proton beam at the rear of the uranium shower plate assembly (TLD Plate 3).

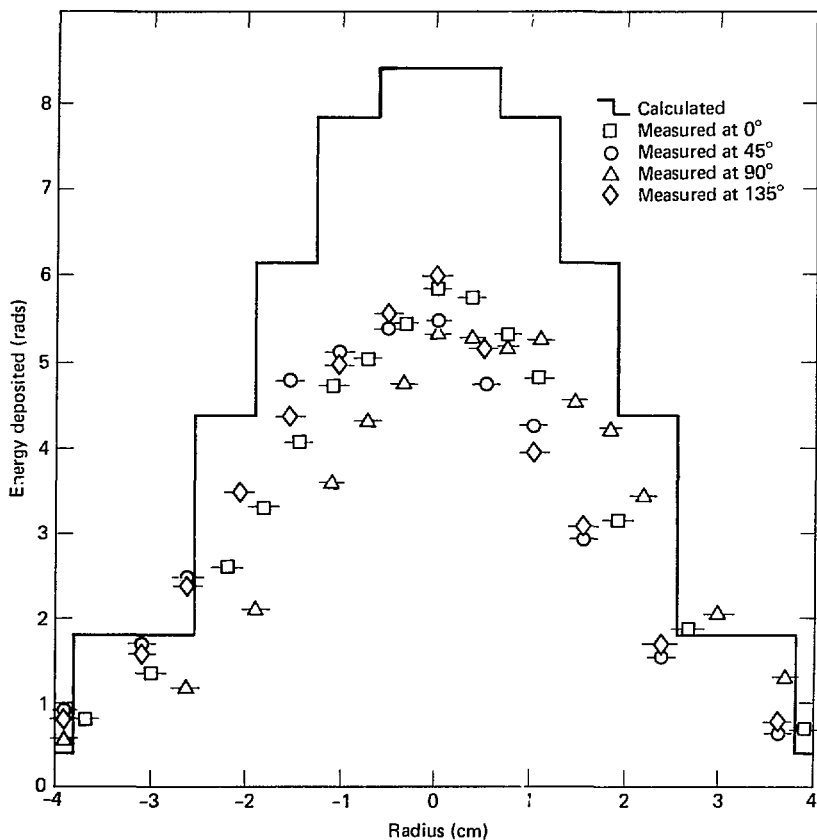


FIG. 10. Energy deposited by a 2.1-GeV proton beam on the front of the polyethylene moderator, behind the air gap (TLD Plate 4).

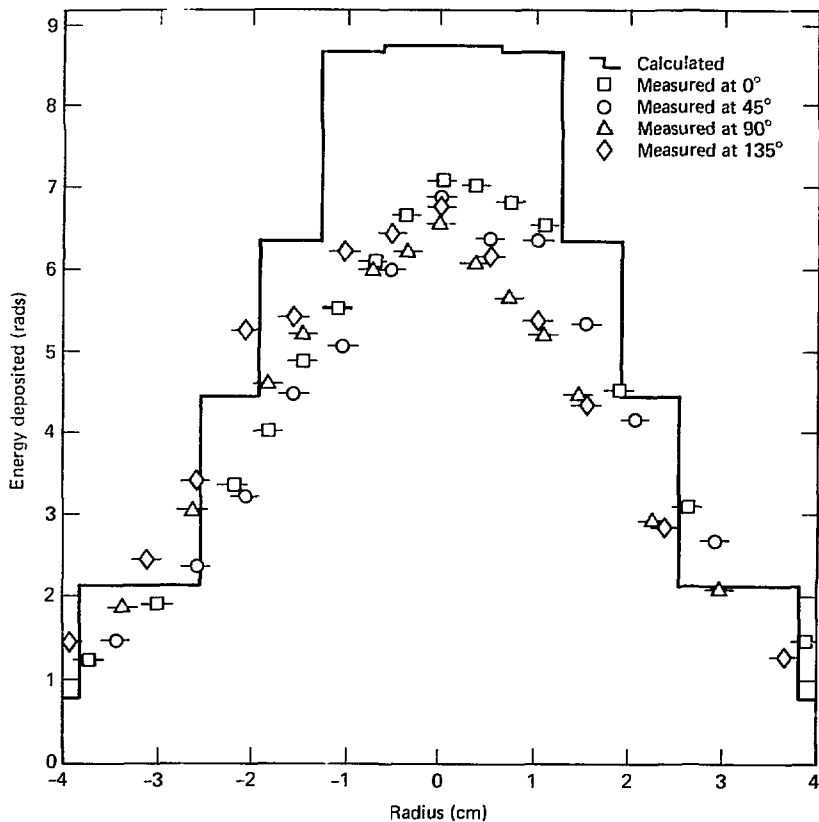


FIG. 11. Energy deposited by a 2.1-GeV proton beam behind the uranium detector plate (TLD Plate 5).

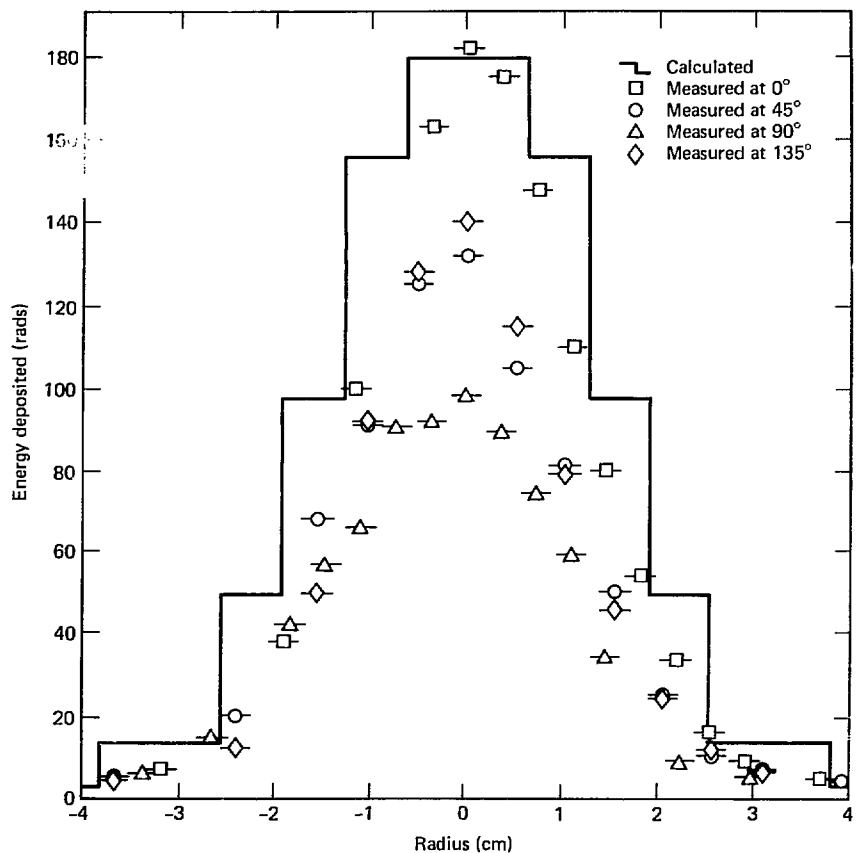


FIG. 12. Energy deposited by a 4.88-GeV proton beam on the front of the uranium shower plate assembly (TLD Plate 1).

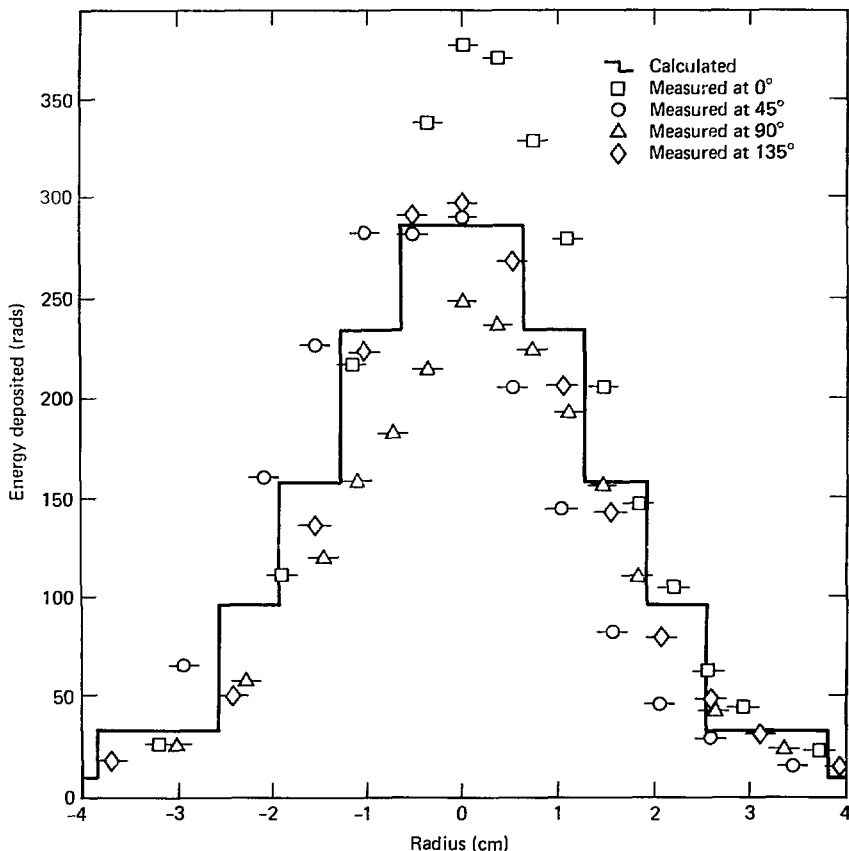


FIG. 13. Energy deposited by a 4.88-GeV proton beam in the middle of the uranium shower plate assembly (TLD Plate 2).

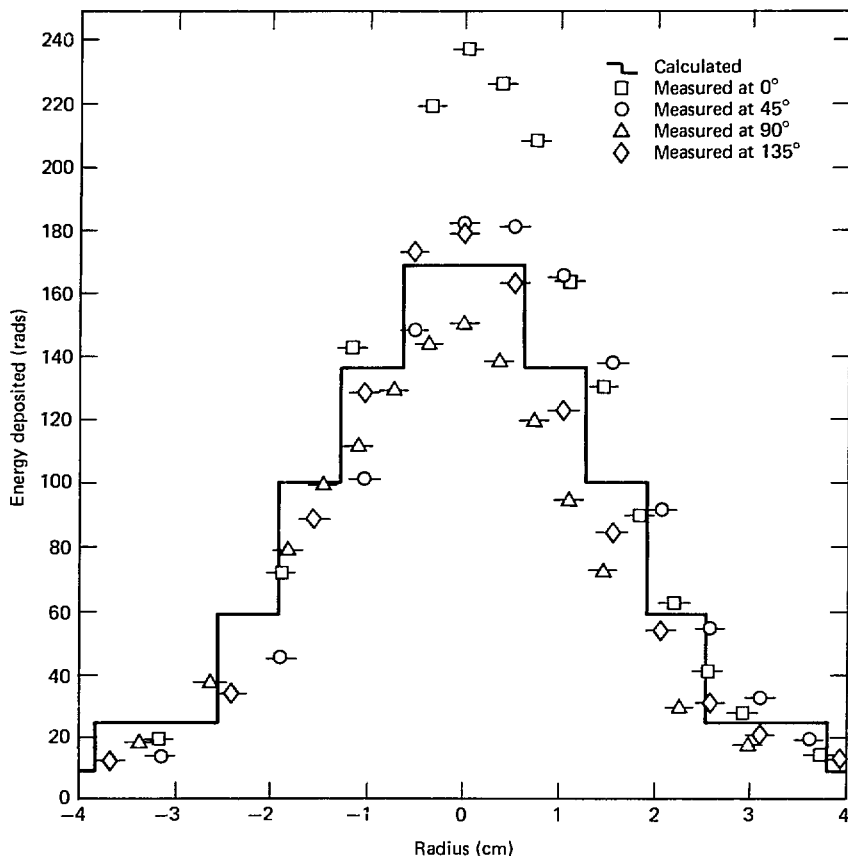


FIG. 14. Energy deposited by a 4.88-GeV proton beam at the rear of the uranium shower plate assembly (TLD Plate 3).

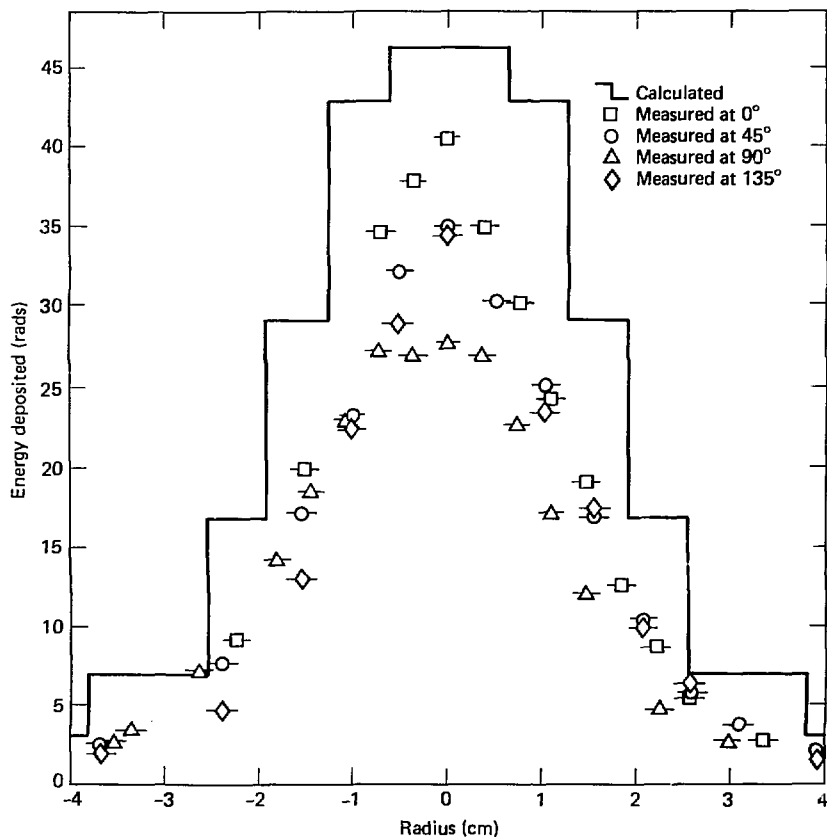


FIG. 15. Energy deposited by a 4.88-GeV proton beam on the front of the polyethylene moderator, behind the air gap (TLD Plate 4).

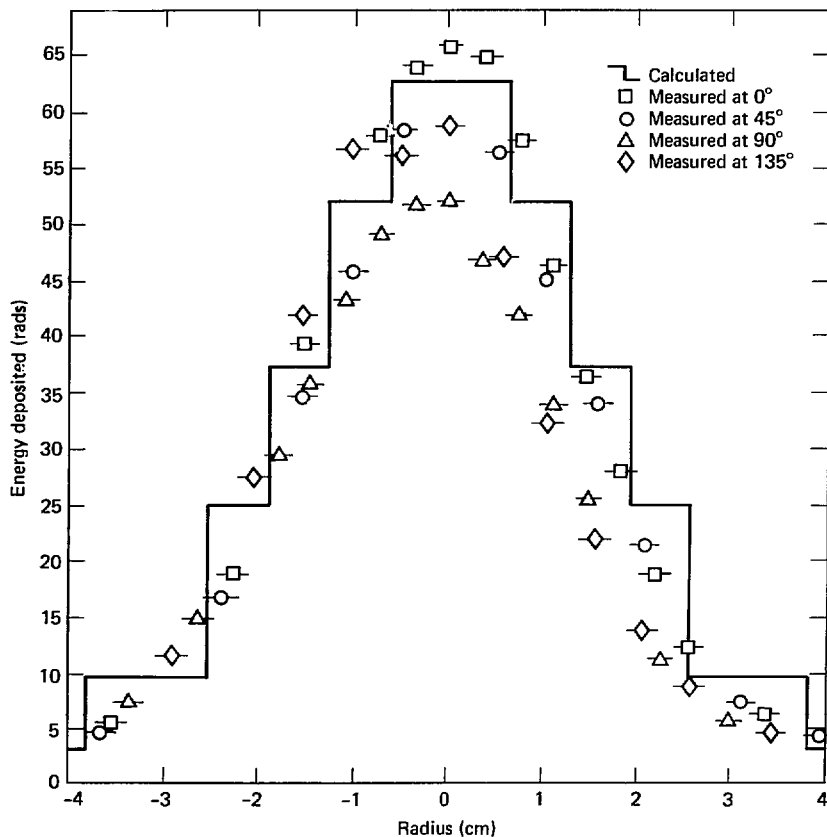


FIG. 16. Energy deposited by a 4.88-GeV proton beam behind the uranium detector plate (TLD Plate 5).

obliterated in Plate 5, apparently by those particles responsible for the phenomenon called buildup.*

The fact that the discrepancy at greater depths persisted at lower beam energies, for which buildup was unimportant, suggests the hypothesis that the primary-beam angular distributions are inadequately modeled in HETC, while the secondary-particle angular distributions (which are largely responsible for the buildup phenomenon) are adequately modeled. However, our study showed that multiple small-angle scattering of the primary protons does not seem to be deficient, as discussed on page 9. It is noteworthy that essentially the same discrepancies are associated with calculations of these experimental configurations by workers at Kaman Nuclear. They used a modified version of CASIM, a computer code wholly independent of HETC, which was written by A. Van Ginneken of Fermilab. Thus, some kind of deficiency in basic physical data may be involved. (See Ref. 4 for further discussion of these comparisons.)

Fission-density comparisons for the 4.88-GeV beam are shown in Fig. 17, where the ordinate units are again calories of fission energy per gram of uranium divided by the delivered beam energy in kilojoules per cm^2 of incident surface ($\text{cal/g}/(\text{kJ}/\text{cm}^2)$). The calculated data are plotted with the center at the center of the experimental assembly, rather than at the maximum experimental value (the presumed beam center) as was done with the figures showing TLD data (for example, Figs. 12-16). Since the calculations are symmetrical, all four calculated surfaces could have been plotted on the x-axis figure

and on the y-axis figure; however, only the A surface is shown on the x-axis figure to allow closer examination of the experimental data. The comparisons shown in Fig. 17, along with the quoted factor-of-two uncertainty in the measured values, suggest that the reliability of the calculated fission-density profiles and magnitudes is probably similar to that of the energy-deposited comparisons with TLD plates (characterized on page 9 as very good, with exceptions).

28.5-GeV BEAM

The deposited-energy comparisons for the 28.5-GeV beam are shown in Figs. 18-22. These comparisons present a confusing picture. Figure 18 suggests a large error in the measurement of beam intensity, but Figs. 19, 20, and 22 show very good agreement. Figure 21 also indicates that the beam calibration was *not* faulty, but the calculated data are somewhat higher relative to the measured results than would have been expected on the basis of the decreased discrepancy shown by the 4.88-GeV data. We have unsuccessfully searched for an explanation in a variety of diagnostic runs with HETC, which break down energy deposited into its constituents.

These 28.5-GeV comparisons are unsettling. It does not seem justifiable to conclude that HETC has failed at this energy, but there certainly is no basis for viewing these results as confirmation of HETC at energies greater than 5 GeV.

SUMMARY OF COMPARISONS

In the range 0.8 to 5 GeV, HETC gives very good values for energy deposited before the air gap and very good radial profiles after the gap, but is defective by 30 to 50% immediately following the gap. HETC values of fission densities are at least approximately correct, and may be much better than that. Data calculated by HETC for higher beam energies must be used with caution if accuracy closer than a factor of two is desired, but suspicion

is not justified. Another experiment at 28.5 GeV would probably resolve this uncertainty.

An over-simplified but useful summarizing comparison is given in Table 2. Measured and

TABLE 2. On-axis energy, in $(\text{cal/g})/(\text{kJ}/\text{cm}^2)$, deposited at rear of polyethylene slab.

| Beam energy, GeV | Measured (M) | Calculated (C) | Ratio, C/M |
|------------------|--------------|----------------|------------|
| 0.8 | 0.030 | 0.040 | 1.32 |
| 2.1 | 0.014 | 0.016 | 1.16 |
| 4.88 | 0.042 | 0.038 | 0.92 |
| 28.5 | 0.017 | 0.012 | 0.69 |

*"Buildup" is a term referring to an excess in energy deposited over what might be expected from simple attenuation of a beam of particles, which can be so large as to cause *increases* in energy deposited at greater depths, as in Figs. 11-13.

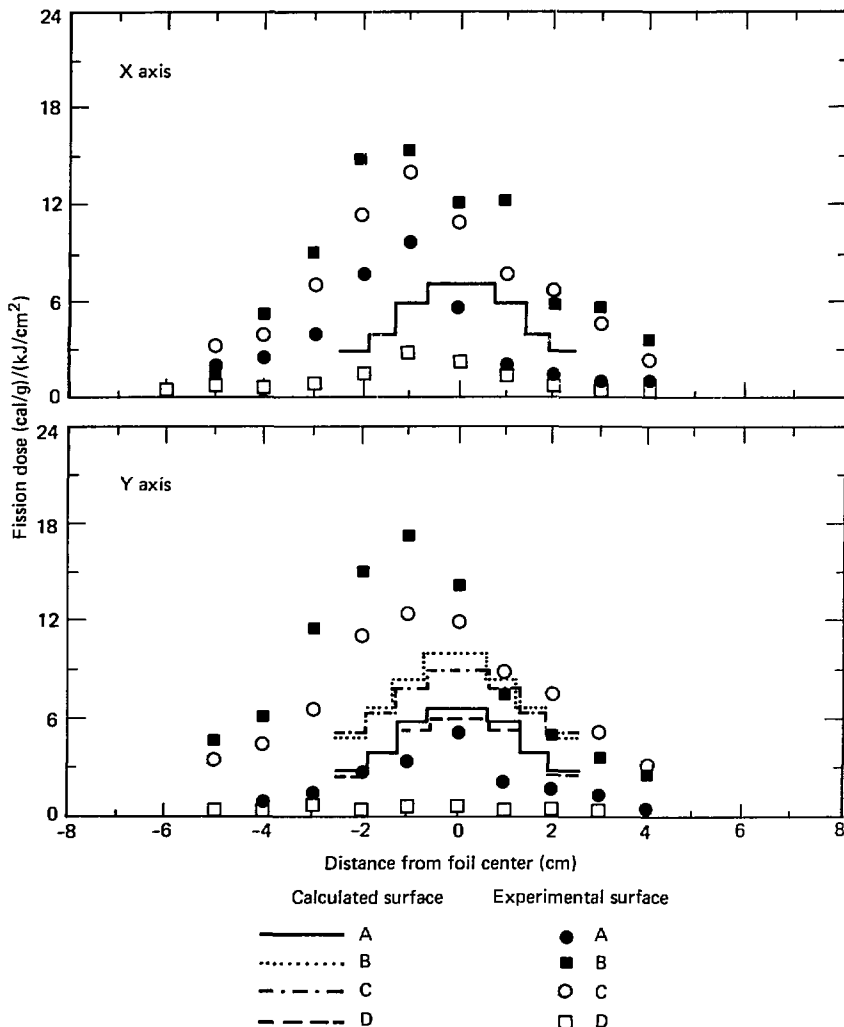


FIG. 17. Fission density distributions, 4.88-GeV proton beam. Each surface is in contact with a uranium plate face. Surface A is adjacent to TLD Plate 1, surfaces B and C are each adjacent to TLD Plate 2, and surface D is adjacent to TLD Plate 3.

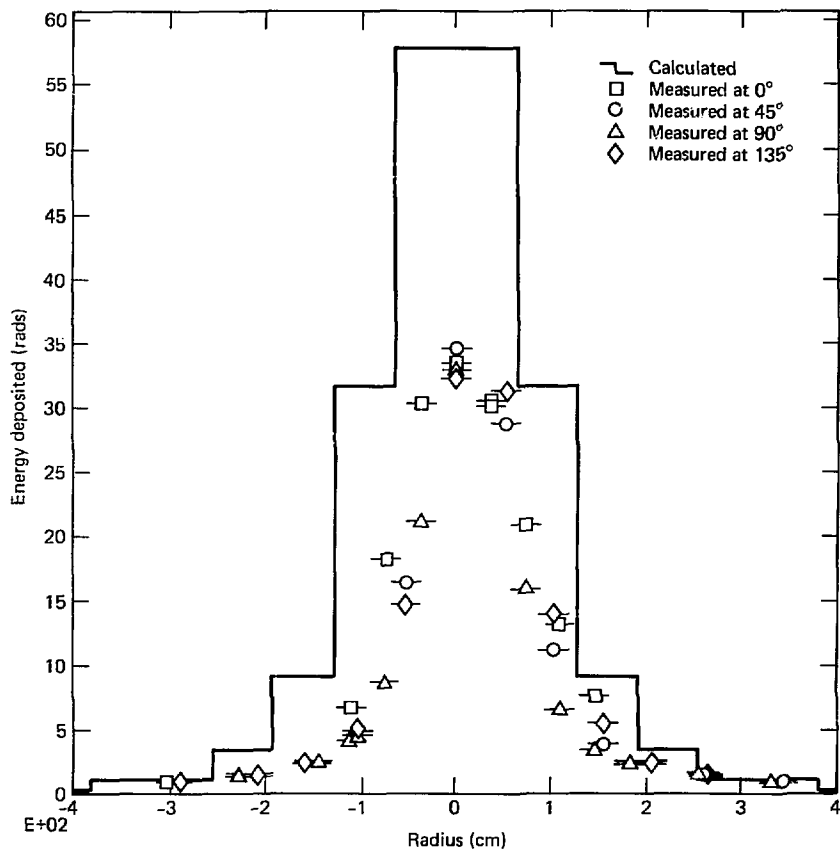


FIG. 18. Energy deposited by a 28.5-GeV proton beam on the front of the uranium shower plate assembly (TLD Plate I).

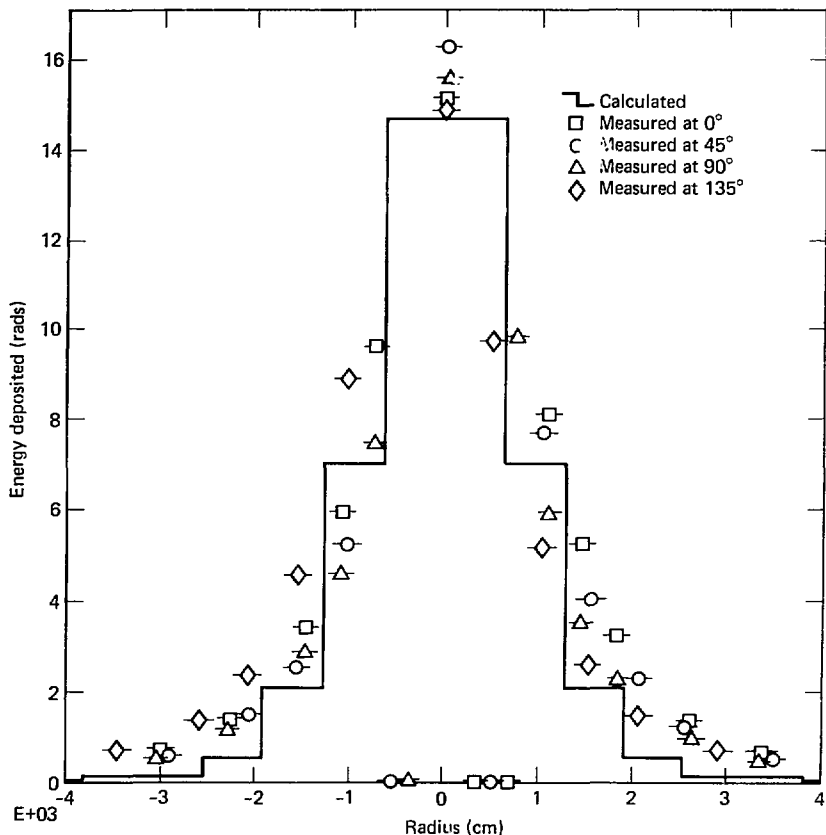


FIG. 19. Energy deposited by a 28.5-GeV proton beam in the middle of the uranium shower plate assembly (TLD Plate 2).

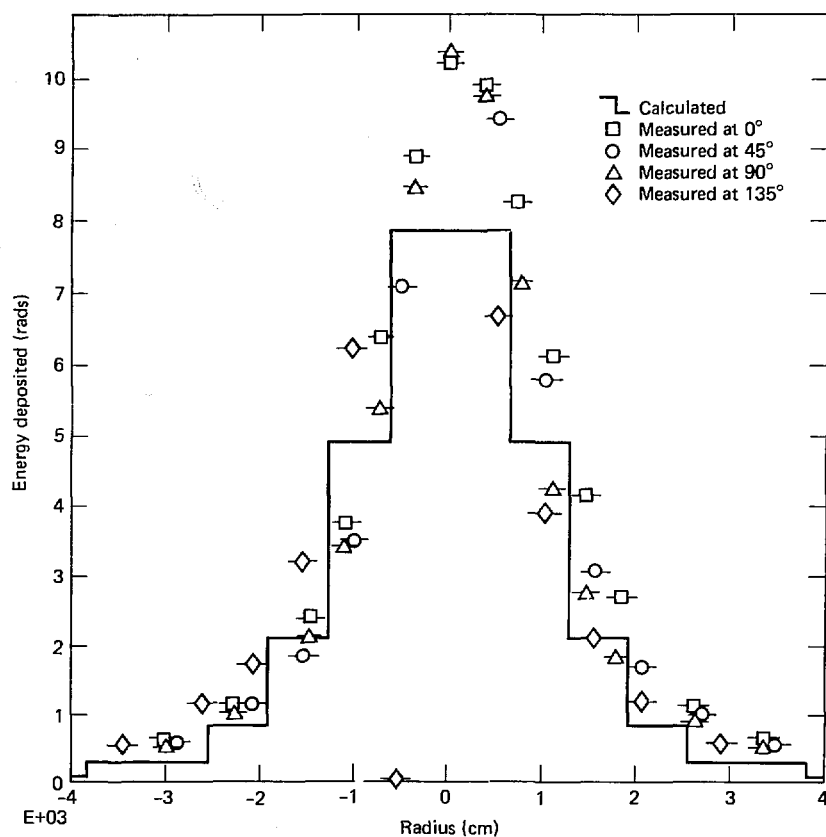


FIG. 20. Energy deposited by a 28.5-GeV proton beam at the rear of the uranium shower plate assembly (TLD Plate 3).

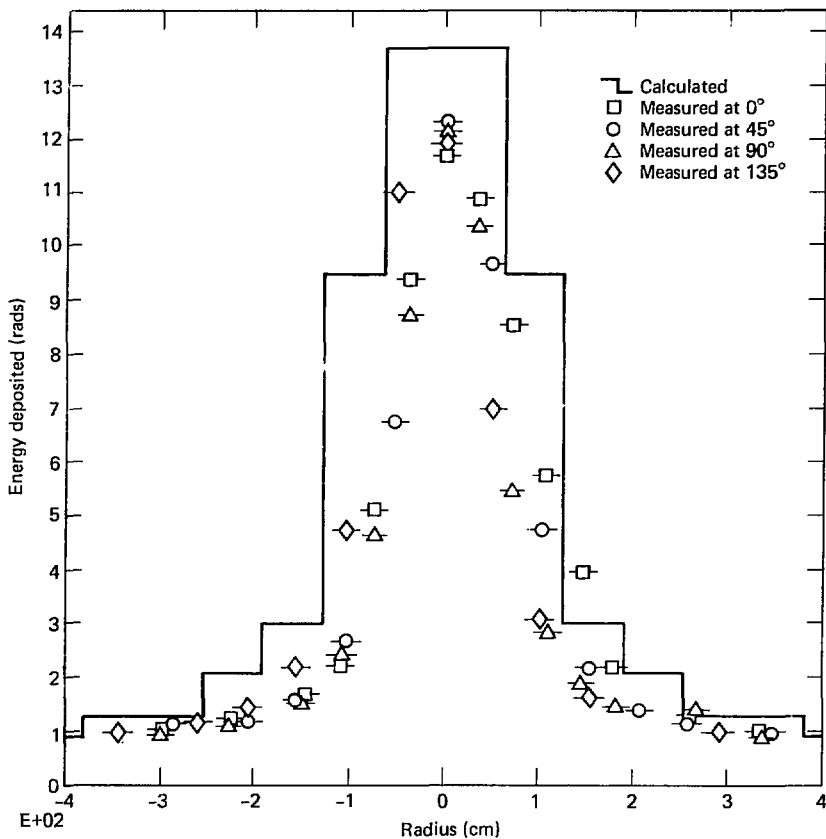


FIG. 21. Energy deposited by a 28.5-GeV proton beam on the front of the polyethylene moderator, behind the air gap (TLD Plate 4).

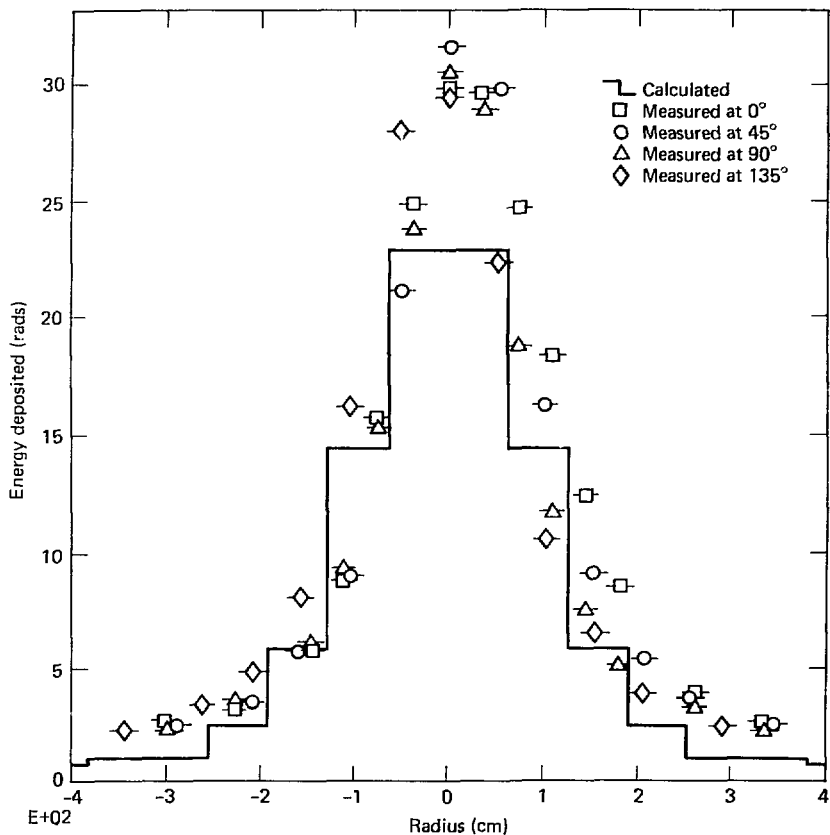


FIG. 22. Energy deposited by a 28.5-GeV proton beam behind the uranium detector plate (TLD Plate 5).

calculated values of energy deposited for all four beam energies are compared at the on-axis position at the very rear of the experimental assembly. Because this position has the poorest calculational statistics and has seen the greatest effect of beam/material interaction, it is among the most difficult locations to calculate.

No adjustments of any kind were made to either the calculations or the measurements. This is the case for all data shown in this report. The agreement, over a range of 30X in energy, is remarkably good.

CONCLUSIONS

For protons in the range 0.8 to 5 GeV, HETC data on energy deposited can be considered accurate to a few tens of percent or better for assemblies similar to the shower-plate part of the LLNL flat plate assemblies, and to better than fifty percent for the moderator/detector plate. The available data neither support nor discredit similar statements about calculated fission density data, which may be presumed to be of similar quality.

At higher energies, HETC data on similar experimental assemblies must be used with caution but not with suspicion.

The 15-inch gap between the shower plate and detector plate provides a severe test of the calculational models, since small angular errors at the shower plate are magnified into large translational errors that appear as amplitudes at the detector plate. Because of this severity, and in view of the overall quality of the comparisons, the agreement between measured and calculated values may be judged excellent, and serves as an absolute validation of the values quoted here for energy deposited in such physical configurations.

ACKNOWLEDGMENTS

This work was made possible by the allocation of resources and encouragement of H. W. Kruger of LLNL. R. G. Alsmiller, Jr. of ORNL was helpful in easing our initial contact with HETC, and T. A. Gabriel of ORNL has provided generous aid throughout this work. W. E. Farley of LLNL has given us his continuing interest and perspective as the experimentalist in charge of the measurements against which our comparisons have been made.

REFERENCES

1. *HETC, Monte Carlo High-Energy Nucleon Transport Code*, Radiation Shielding Information Center, Oak Ridge National Laboratory, Oak Ridge, TN, CCC-178 (1970).
2. K. Crase, W. E. Farley, H. Kruger, D. Selway, and G. S. Sidhu, *Measurement of Energy Deposited by Charged Particle Beams in Composite Targets*, Lawrence Livermore National Laboratory, Livermore, CA, UCRL-52459 (1977).
3. T. P. Wilcox, *MORSE-L, A Special Version of the MORSE Program Designed to Solve Neutron, Gamma and Coupled Neutron-Gamma Penetration Problems*, Lawrence Livermore National Laboratory, Livermore, CA, UCID-16680 (1972). (MORSE itself is a Monte Carlo code written at ORNL.)
4. W. E. Loewe, *Comparison between Calculation and Measurement of Energy Deposited by 800 MeV Protons*, Lawrence Livermore National Laboratory, Livermore, CA, UCID-18634 (1980).